

Published in final edited form as:

Bioorg Chem. 2010 October ; 38(5): 224–228. doi:10.1016/j.bioorg.2010.05.003.

The rate of spontaneous cleavage of the glycosidic bond of adenosine

Randy B. Stockbridge, Gottfried K. Schroeder, and Richard Wolfenden *

Department of Biochemistry and Biophysics, University of North Carolina at Chapel Hill, Chapel Hill, North Carolina 27599

Abstract

Previous estimates of the rate of spontaneous cleavage of the glycosidic bond of adenosine were determined by extrapolating the rates of the acid - and base-catalyzed reactions to neutral pH. Here we show that cleavage also proceeds through a pH-independent mechanism. Rate constants were determined as a function of temperature at pH 7 and a linear Arrhenius plot was constructed. Uncatalyzed cleavage occurs with a rate constant of $3.7 \times 10^{-12} \text{ s}^{-1}$ at 25 °C, and the rate enhancement generated by the corresponding glycoside hydrolase is $\sim 5 \times 10^{12}$ -fold.

Keywords

adenosine; nucleoside N-ribohydrolase; ricin; thermodynamics of activation; rate enhancement; glycoside cleavage

1. Introduction

Enzymes that catalyze the hydrolysis of the N-glycoside bonds of ribonucleosides are required for ribonucleoside salvage and tRNA modification. The mammalian enzymes that catalyze N-glycosidic bond cleavage involve covalent intermediates (tRN A transglycosylases, [1]) or substrate activation by exogenous anions (purine nucleoside phosphorylases, [2]), but some plants [3], protists [4], and bacteria [5] possess enzymes that catalyze the direct hydrolysis of the glycoside bond. Trypanosomes, including the parasites that cause sleeping sickness in humans and livestock in sub-Saharan Africa, lack a *de novo* purine synthesis pathway and instead scavenge purine ribonucleosides from their mammalian hosts [6]. These parasites convert the purine ribonucleosides to purines using nucleoside N-ribohydrolases that differ substantially from the purine nucleoside phosphorylases of mammalian purine salvage [2]. Plant-derived ribosome-inactivating proteins, including ricin A-chain, also have ribohydrolytic activity. Ricin halts translation by catalyzing the depurination of a single adenosine residue in the ribosomal RNA [7].

Enzymes that furnish large rate enhancements are especially sensitive to inhibition [8]. Thus, information about the rate of the uncatalyzed hydrolysis of ribonucleosides would be useful in estimating the potential binding affinities of transition state analogs of these

*Address correspondence to: Richard Wolfenden, PhD, 120 Mason Farm Rd, Genetic Medicine Suite 3010, Chapel Hill, North Carolina, 27599. Phone: 919-966-1203. Fax: 919-966-2852; water@med.unc.edu.

Publisher's Disclaimer: This is a PDF file of an unedited manuscript that has been accepted for publication. As a service to our customers we are providing this early version of the manuscript. The manuscript will undergo copyediting, typesetting, and review of the resulting proof before it is published in its final citable form. Please note that during the production process errors may be discovered which could affect the content, and all legal disclaimers that apply to the journal pertain.

enzymes. For both ricin and purine nucleoside ribohydrolases, effective inhibitors have been designed by analogy to acid-catalyzed glycosidic bond hydrolysis [9]. Kinetic isotope effects on the adenosine N7 and C1' atoms for acid-catalyzed and enzymatic purine hydrolysis indicate that the mechanisms are similar and involve protonation at N7 (~-1.6 [10]) followed by nucleophile attack at C1' [4,11,12].

However, the rate of adenosine hydrolysis at pH 7 – and thus the rate enhancements provided by ricin and purine nucleoside N-ribohydrolases, which act on their natural substrates at neutral pH – does not appear to have been established. Adenosine hydrolysis is catalyzed by both acid and base [13,14,15], and the rate of hydrolysis at pH 7 has been estimated by adding the extrapolated rate constants of the H⁺ and OH⁻-catalyzed reactions [14]. But those data were obtained over a relatively narrow pH range, and rate constants have not been measured at pH 7 (Figure 1). Thus, it is not known whether the rate equation includes a term for the uncatalyzed hydrolysis of adenosine, or, alternatively, whether the observed rate at pH 7 is a composite of the rate terms for acid- and base-catalyzed glycosidic bond cleavage in roughly equal proportions. To the extent that the base-catalyzed reaction contributes to the observed rate constant at pH 7, it would not be a good model for the enzymatic reaction because it proceeds through an indirect mechanism that involves formation of an N6-ribosyl adenine intermediate and opening of the imidazole moiety of the adenine ring [15].

In the present work, we conducted experiments at elevated temperatures to establish whether uncatalyzed glycosidic bond cleavage occurs. We show that a pH-independent term exists in the rate equation for adenosine hydrolysis, and that the rate enhancement generated by adenine nucleoside hydrolases is ~5 × 10¹²-fold.

2. Materials and Methods

Reagents were obtained from Sigma-Aldrich Co. In a typical experiment, adenosine (.015 M) and an anionic buffer (0.1 M) were sealed in quartz tubes under vacuum and incubated in convection ovens (Barnsted/Thermolyne Corp., model 47900) at temperatures between 110 and 190 °C for varying lengths of time. Buffers used were sodium arsenate (pH 2.3–3.4, pH 7.0–7.2, and pH 10.5–10.7), potassium formate (pH 3.4–4.7), potassium acetate (pH 4.6–5.3), potassium phosphate (pH 6.2–7.0), ethyl phosphonate (pH 7.3–8.4), and sodium carbonate (pH 9.6–10.4). After reaction, samples were mixed with D₂O containing 0.1 M phosphate buffer (pH 6.8) and pyrazine (4 H, $\delta = 8.6$, 1 × 10⁻³ M) as an internal integration standard. ¹H NMR spectra were obtained immediately after admixture with D₂O. Separate experiments monitoring the exchange of adenine protons with D₂O that after 1 hour ~1% of the adenine protons had exchanged. Data were acquired using a Varian 500 MHz spectrometer with a cold probe for a minimum of 4 transients using a standard water suppression pulse sequence. Spectra were analyzed offline using Spinworks [16]. The integrated intensities of the peaks arising from the anomeric (C1) proton of adenosine and the C2 and C8 protons of adenine were used to determine the extent of reaction. Reaction mixtures (diluted 1000-fold) were also analyzed spectrophotometrically in the UV range using a Hewlett-Packard 8452A diode array spectrophotometer.

Prior to ¹H NMR identification, adenine β -ribofuranoside (the starting material), adenine, adenine α -ribofuranoside, adenine α -ribofuranoside, and adenine β -ribofuranoside were isolated by HPLC on a reverse phase C18 column (Whatman Partisil ODS3). Elution was performed isocratically with 0.05 M potassium phosphate (pH 5.4) and 5% methanol at a flow rate of 1 mL/min. Adenine, adenine α -ribofuranoside, and adenine β -ribofuranoside eluted after 15 minutes, and adenine β -ribofuranoside and adenine α -ribofuranoside eluted after 25 minutes.

3. Results

3.1 pH profile

Adenosine decomposition was monitored at 130 °C in anionic buffers (0.1 M) ranging between pH 1.2 and pH 10.7 (pH measured at 25 °C). Separate experiments showed that the effect of ionic strength on the rate of glycosidic bond cleavage is modest. The rate increased by ~2-fold as the concentration of potassium chloride increased from 0–1.0 M. The rate of glycosidic bond cleavage was determined based on the appearance of adenine using ¹H NMR. Separate experiments showed adenine to be stable at 130 °C for the lengths of time at the pH values over which data were gathered. In a plot of the logarithm of the rate versus pH (Figure 2A), the slopes of the best fit lines in the acid range (pH 1.2–pH 4.7) and the basic ranges (pH 9.6–pH 10.7) are –0.93 and +0.96 respectively, very close to the values –1.0 and +1.0 expected for acid- and base-catalyzed reactions.

When these lines are extrapolated to pH 7, the logarithm of the rate of the acid-catalyzed reaction is –7.66 with a standard error of ±0.482 logarithmic units. The logarithm of the base-catalyzed reaction at pH 7 is –7.57 with a standard error of ±0.381 logarithmic units. The sum of the extrapolated rate constants of the acid- and base-catalyzed reactions is $4.9 \times 10^{-8} \text{ s}^{-1}$ (log k = –7.31 with a combined standard error of ±0.43 logarithmic units). That value is smaller than the rate of glycosidic bond cleavage that was determined at pH 7 from six independent measurements, $1.1 \times 10^{-6} \text{ s}^{-1}$ (log k = –5.94 with a standard deviation of ±0.08 logarithmic units). Using the hypothesis test for the difference between two means, the difference between the measured rate of glycosidic bond cleavage and the rate expected for the sums of acid- and base-catalyzed glycoside bond cleavage at pH 7 is significant with $p < 0.005$. These findings indicate the presence of an uncatalyzed reaction at neutral pH that proceeds with a rate constant of $1.1 (\pm 0.3) \times 10^{-6} \text{ s}^{-1}$ at 130 °C.

The observed rate constant for glycosidic bond hydrolysis at 130 °C is given by:

$$k_{\text{obs}} = k_{\text{acid}} \cdot [\text{H}^+] + k_{\text{base}} \cdot [\text{OH}^-] + k_{\text{uncat}} \quad (\text{Eq. 1})$$

where k_{acid} ($0.076 \text{ s}^{-1}\text{M}^{-1}$) and ($4.7 \times 10^{-4} \text{ s}^{-1}\text{M}^{-1}$) were determined from the values of the linear fits to data points in the acidic and basic ranges shown in Figure 2A at pH 0 and 11.4 (pK_{w} at 130 °C), respectively. As noted above, k_{uncat} is equal to $1.1 \times 10^{-6} \text{ s}^{-1}$. $[\text{H}^+]$ is equal to $10^{-\text{pH}}$ and $[\text{OH}^-]$ is equal to $10^{\text{pH}-11.4}$. Figure 2B shows the data points from Figure 2A along with a solid line based on Eq. 1 for k_{obs} .

3.2 Adenosine decomposition at pH 7

The time course of adenosine decomposition at pH 7 was monitored over 24 hours at 150 °C using UV spectroscopy (Figure 3A) and ¹H NMR (Figure 3B). UV spectra show that for the first ~50% of the reaction, the amount of adenosine decreases and the amount of adenine increases concomitantly. The overlaid spectra show clean isosbestic points (Figure 3) indicating that glycosidic bond cleavage proceeds without the accumulation of an intermediate in which the adenine ring has opened. In contrast, isosbestic points were not observed for the decomposition of adenosine in alkaline solution, and the mechanism for base-catalyzed hydrolysis was proposed partly on that basis [14, 15]. This qualitative observation provides additional evidence that the reaction at neutral pH does not include a significant contribution from the base-catalyzed reaction, and therefore that the neutral reaction is distinct from the sum of the acid- and base-catalyzed reactions.

At early timepoints in the reaction, five major products were observed by ¹H NMR: adenine, ribose, adenine α -ribofuranoside ($\text{H1}' \delta=6.3, \text{d}$), adenine β -ribofuranoside ($\text{H1}' \delta=5.65, \text{d}$),

and a fifth compound with a peak in the anomeric region believed to be adenine α -ribosepyranoside. The identity of α -adenine ribofuranoside was confirmed by addition of the authentic compound, and the β -adenine ribopyranoside was identified by comparison of the ^1H NMR and ^{13}C NMR spectra with published chemical shifts [15]. The fourth product was isolated by HPLC and appears to be α -adenine ribopyranoside on the basis of its ^1H NMR chemical shifts (Table 1). Thus, the resonance of its putative anomeric proton ($\delta=5.80$, s) is shifted upfield from those of the two adenine ribofuranosides ($\delta=6.34$; $\delta=5.95$), as expected for a ribopyranoside, but downfield from the β -ribosepyranoside ($\delta=5.68$), as expected for an α -ribosepyranoside [17]. The chemical shifts of the anomeric protons of ribose pyranosides tend to exhibit very small coupling constants, and are sometimes collapsed into a singlet [18]. If the ribose ring were to open, then the β -ribosepyranoside starting material or any of three additional anomers might be formed by its reclosure. We observe that the α -ribosepyranoside, β -ribosepyranoside, and probable α -ribosepyranoside were all formed at similar rates and with qualitatively similar activation parameters (Table 1). Similarly, thermal decomposition of the α -ribosepyranoside yielded adenine, and three adenosine anomers (the β -ribosepyranoside, the β -ribosepyranoside, and the α -ribosepyranoside), at comparable rates.

It is probable that each of the four adenosine anomers undergoes hydrolysis to yield adenine. The concentrations of the α -ribosepyranoside, the β -ribosepyranoside, and the probable α -ribosepyranoside rise and fall together over the reaction time course as intermediates. Because glycosidic bond cleavage of each anomer should contribute to the overall rate of adenine formation, rates were determined by measuring the rate of appearance of adenine and the adenosine anomers in the first 10% of the reaction, when the adenosine β -ribosepyranoside starting material was still ~ 30 times more prevalent than any other anomer.

Other peaks are visible in the ^1H NMR spectrum, but they do not appear until after the five initial products described earlier have begun to accumulate (Figure 3B). Because they are not derived from the adenosine starting material, and adenine is thermally stable at pH 7, these other products presumably result from the breakdown of the adenine derivative with an open ribose ring. Importantly, N6-ribosepyranosyl adenines and triaminopyrimidine present in the ^1H NMR spectra of the base-catalyzed reaction are absent in the reaction at pH 7.

3.3 Arrhenius plots

The rates of glycosidic bond cleavage at pH 7 were determined at twelve different temperatures between 110 and 190 °C. A linear Arrhenius plot (Figure 4) was extrapolated to yield a rate constant of $3.7 (\pm 1.3) \times 10^{-12} \text{ s}^{-1}$ at 25 °C, equivalent to a half-time of ~ 6000 years. The thermodynamics of activation were also determined from the Arrhenius plot: $\Delta H^\ddagger = 28.0 \text{ kcal./mol}$, $T\Delta S^\ddagger = -4.9 \text{ kcal./mol}$, and $\Delta G^\ddagger = 32.9 \pm 0.3 \text{ kcal./mol}$.¹

4. Discussion and Conclusions

4.1 Presence of an uncatalyzed reaction

Three lines of evidence indicate the existence of uncatalyzed glycosidic bond hydrolysis at pH 7. First, at 130 °C, the observed reaction rate at pH 7 is greater than the sum of the acid- and base-catalyzed reactions by a factor of 23. That difference is statistically significant with

¹From ΔG^\ddagger and ΔH^\ddagger values reported for the acid- and base-catalyzed reactions [13,14], k_{uncat} was expected to be the dominant term in the rate equation at pH 7 over the range of temperatures that data were collected. At 110 °C, $\Delta G^\ddagger \sim 29.4 \text{ kcal./mol}$ for the acid-catalyzed reaction, $\sim 28.7 \text{ kcal./mol}$ for the base-catalyzed reaction, and $\sim 26.6 \text{ kcal./mol}$ for the neutral reaction. At 190 °C, $\Delta G^\ddagger \sim 26.0 \text{ kcal./mol}$ for the acid-catalyzed reaction, $\sim 26.6 \text{ kcal./mol}$ for the base-catalyzed reaction, and $\sim 22.7 \text{ kcal./mol}$ for the neutral reaction. At 25 °C, the base-catalyzed reaction might be expected to contribute to the observed rate constant, with $\Delta G^\ddagger \sim 35.0$ for the acid-catalyzed reaction, $\Delta G^\ddagger \sim 32.1$ for the base-catalyzed reaction, and $\Delta G^\ddagger \sim 32.9$ for the neutral reaction. However, extrapolation of the Arrhenius plot is expected to yield an accurate estimate of k_{uncat} at 25 °C.

$p < 0.005$. Second, an isosbestic point is observed by UV spectroscopy at pH 7, but not at alkaline pH. Thus, the observed UV spectra are not consistent with a composite reaction to which the base-catalyzed reaction contributes significantly. Third, the base-catalyzed reaction yields a number of products that can be observed in the ^1H NMR spectrum including N6-ribosyl derivatives of adenine and triaminopyrimidine. These products were not observed for the reaction at pH 7, which also tends to suggest that the rate constants measured at pH 7 are for a third, uncatalyzed, reaction rather than for the combined acid- and base-catalyzed reactions.

4.2 Mechanism of adenosine decomposition at pH 7

At pH 7, the adenine β -ribofuranoside starting material can decompose by two principal pathways. In the first, adenosine undergoes simple glycosidic bond hydrolysis to yield adenine and ribose. The present results indicate that glycosidic bond cleavage proceeds through an acid- and base-independent mechanism that does not involve opening the adenine ring. Alternatively, the ribose ring could open and re-close, yielding any of the other adenosine anomers: the α -furanoside, and the α - and β -pyranosides.

Opening of the ribose ring was not observed in acid or base. To our knowledge, this is the first time that the α -furanoside and α -pyranoside have been obtained by the thermal degradation of adenine β -ribofuranoside. Since it is likely that the open ribose ring also re-closes to form the β -furanoside starting material, it is not possible to determine the rate of ribose ring-opening from these experiments. However, the sum of the rate constants of formation of the other three anomers is similar in magnitude to the rate constants of adenine formation, so it appears that ribose ring-opening and glycosidic bond hydrolysis occur at similar rates.

Further kinetic analysis will be required to resolve the detailed mechanism of adenosine decomposition at pH 7. It seems probable that both glycosidic bond hydrolysis and anomerization involve the development of positive charge at the anomeric carbon. Such charge development is consistent with the small increase in rate produced by an increase in ionic strength. A carbocation at C1' and coplanar intermediate would be required to allow rotation of H1' and the adenine moiety to form the α -adenosine anomers. For glycosidic bond cleavage, a build up of positive charge on C1' has been predicted for the enzymatic glycosidic bond cleavages catalyzed by trypanosomal nucleoside hydrolase [4] and ricin A-chain (for which a carbocation intermediate bearing a full charge was proposed, [12]) on the basis of kinetic isotope effects on C1'. It seems likely that the neutral reaction would behave similarly, although the details of proton transfer from water to adenine are not clear at this time.

4.3 Rate enhancements generated by nucleoside hydrolases

Comparison of rate constants observed for enzyme-catalyzed and uncatalyzed reactions allows the rate enhancement, rate $k_{\text{cat}}/k_{\text{non}}$, to be estimated. The reported constants are 30 s^{-1} for ricin A-chain [19] and 18 s^{-1} for *Trypanosoma brucei* nucleoside ribohydrolase [6]. Thus, the rate enhancement produced by both enzymes is $\sim 5 \times 10^{12}$, and these enzymes are among the more proficient hydrolases that have been described [8].

It is also of interest to compare the rate enhancements generated by enzymes that catalyze adenosine and deoxyadenosine hydrolysis at neutral pH. Uncatalyzed adenosine hydrolysis proceeds at a rate that is ~ 30 -fold slower than that previously reported for deoxyadenosine hydrolysis [20]. (That effect of the 2' OH group on uncatalyzed glycosidic bond hydrolysis is somewhat less than the 650-fold effect that it exerts on acid-catalyzed glycosidic bond cleavage [21].) Since many DNA glycosylases exhibit rate constants below 1 s^{-1} [20], these

enzymes are less proficient than enzymes involved in adenosine glycosidic bond cleavage (Table 2). A quick turnover is probably less important for enzymes involved in editing functions such as DNA excision and repair.

Acknowledgments

We thank Laura Hall for performing preliminary HPLC separations of the adenosine anomers. This work was supported by NIH grant GM -18325.

References

1. Romier C, Reuter K, Suck D, Ficner R. *Biochemistry* 1996;35:15734–15739. [PubMed: 8961936]
2. Parkin DW, Horenstein BA, Abdulah DR, Estupinan B, Schramm VL. *J Biol Chem* 1991;31:20658–20665. [PubMed: 1939115]
3. Jung B, Florchinger M, Kunz HH, Traub M, Wartenberg R, Jeblick W, Neuhaus HE, Mohlmann T. *Plant Cell* 2009;21:876–891. [PubMed: 19293370]
4. Horenstein BA, Parkin DW, Estupinan B, Schramm VL. *Biochemistry* 1991;30:10788–10795. [PubMed: 1931998]
5. Giabbai B, Degano M. *Structure* 2004;12:739–749. [PubMed: 15130467]
6. Parkin DW. *J Biol Chem* 1996;271:21713–21719. [PubMed: 8702965]
7. Endo Y, Mitsui K, Motizuki K, Tsurugi K. *J Biol Chem* 1987;262:5908–5912. [PubMed: 3571242]
8. Wolfenden R. *Chem Rev* 2006;106:3379–3396. [PubMed: 16895333]
9. Schramm VL. *Nucleic Acids Res Suppl* 2003;3:107–108.
10. Kim S, Martin RB. *Inorganica Chimica Acta* 1984;91:19–24.
11. Parkin DW, Leung HB, Schramm VL. *J Biol Chem* 1984;259:9411–9417. [PubMed: 6746654]
12. Chen XY, Berti PJ, Schramm VL. *J Am Chem Soc* 2000;122:1609–1617.
13. Garrett ER, Mehta PJ. *J Am Chem Soc* 1972;94:8532–8541. [PubMed: 4638983]
14. Garrett ER, Mehta PJ. *J Am Chem Soc* 1972;94:8542–8547. [PubMed: 4638984]
15. Lehikoinen P, Mattinen J, Lonnberg H. *J Org Chem* 1986;51:3819–3823.
16. Marat, K. Spinworks, version 2.5.2. University of Manitoba; Winnipeg, MB: 1999–2007.
17. Altona C, Sundaralingam M. *J Am Chem Soc* 1973;95:2333–2344. [PubMed: 4709237]
18. Kotowycz G, Lemieux RU. *Chem Rev* 1973;73:669–698.
19. Endo Y, Tsurugi K. *J Biol Chem* 1988;263:8735–8739. [PubMed: 3288622]
20. Schroeder GK, Wolfenden R. *Biochemistry* 2007;46:13638–13647. [PubMed: 17973496]
21. Venner HZ. *Physiol Chem* 1964;339:14–27.
22. Ciuffreda P, Casati S, Manzocchi A. *Magnetic Resonance in Chem* 2007;45:781–784.
23. Noll DM, Gogos A, Granek JA, Clarke ND. *Biochemistry* 1999;38:6374–6379. [PubMed: 10350454]

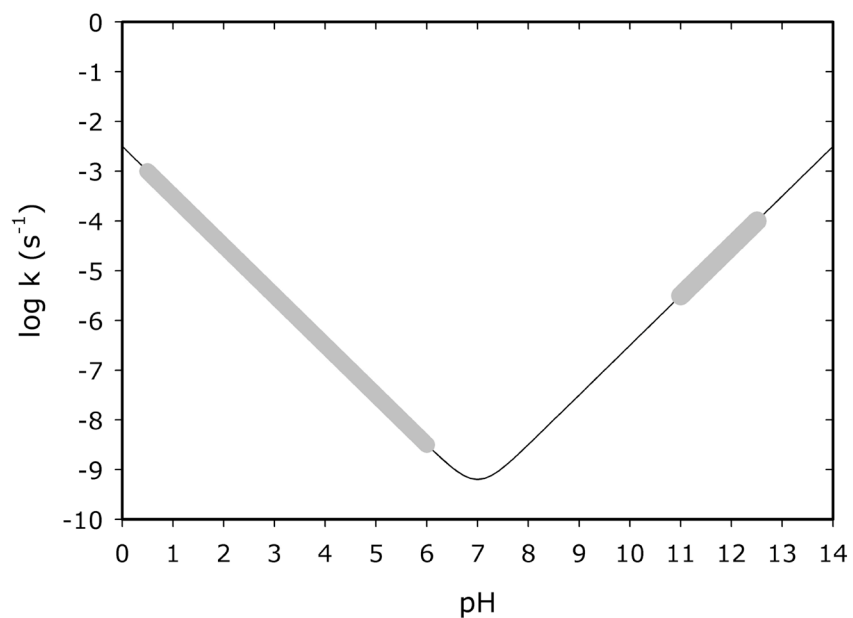


Figure 1. Representation of the pH profile used by Garrett and Mehta [14] to estimate the rate of adenosine cleavage at pH 7. Data were collected at 80 °C over the pH range indicated by the gray bars. The solid line represents the extrapolation of those data.

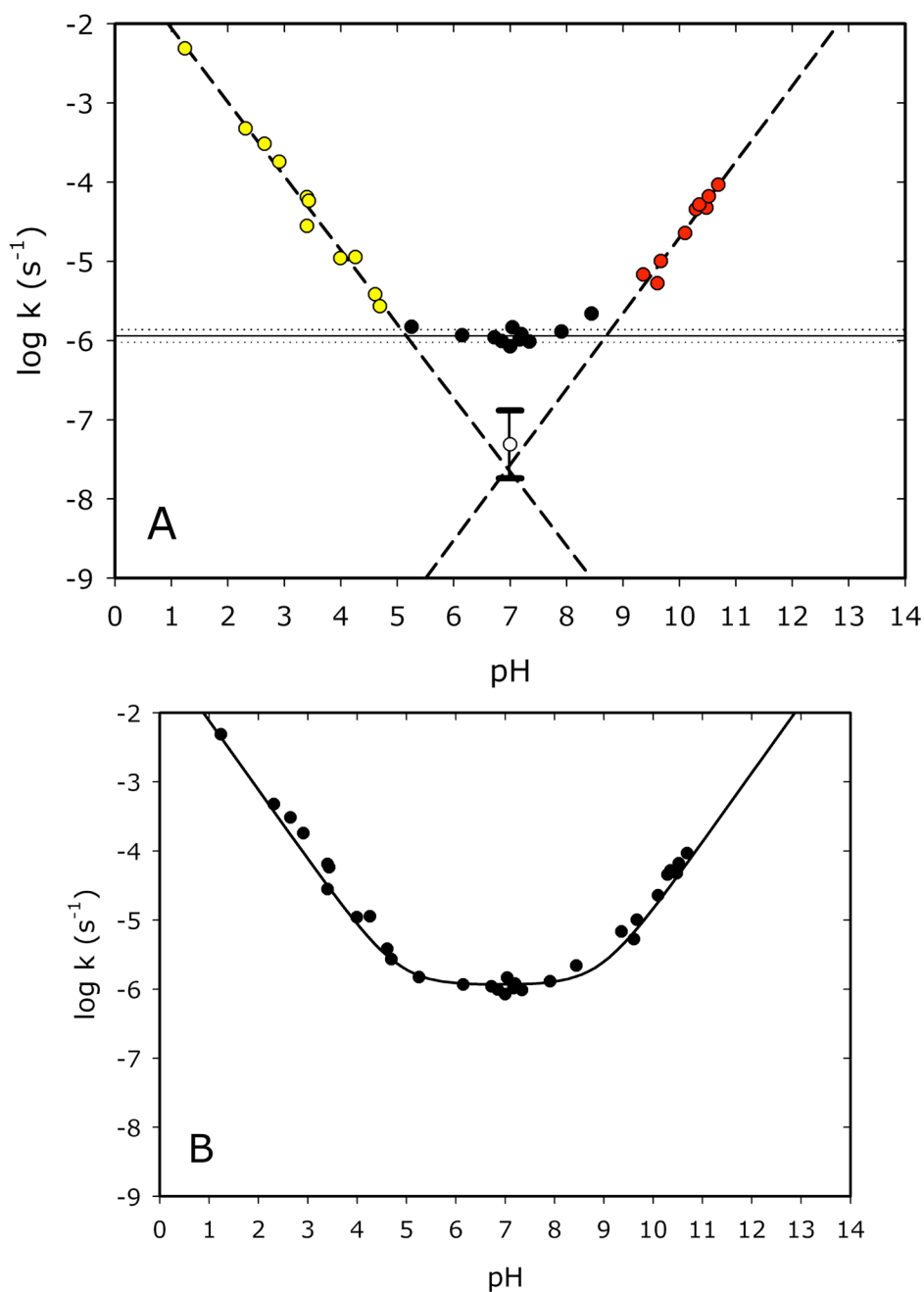


Figure 2.

The logarithm of the rate (s^{-1}) of adenine formation from adenosine versus pH at 130 °C (pH values determined at 25 °C). (A) Points used to determine the acid - and base- catalyzed rates are shown in yellow (pH values 1.0 – 4.6) and red (pH values 9.2 – 11.0), respectively. The linear regressions fit to those points are shown as dashed lines. The mean value for rate determined at pH 7 by the solid horizontal line (k_{uncat}) is indicated at $x = -5.94$. The standard error for the measurement of k_{uncat} is indicated by the shaded area. The sum of the extrapolated acid - and base-catalyzed rates at pH 7 is indicated by the open point at pH 7. The standard error for the extrapolation is indicated by the error bars. (B) Data points with a

solid line that represents the theoretical expression for k_{obs} , comprised of calculated rate constants for, k_{acid} , k_{base} , and k_{uncat} (see section 3.1, Eq. 1).

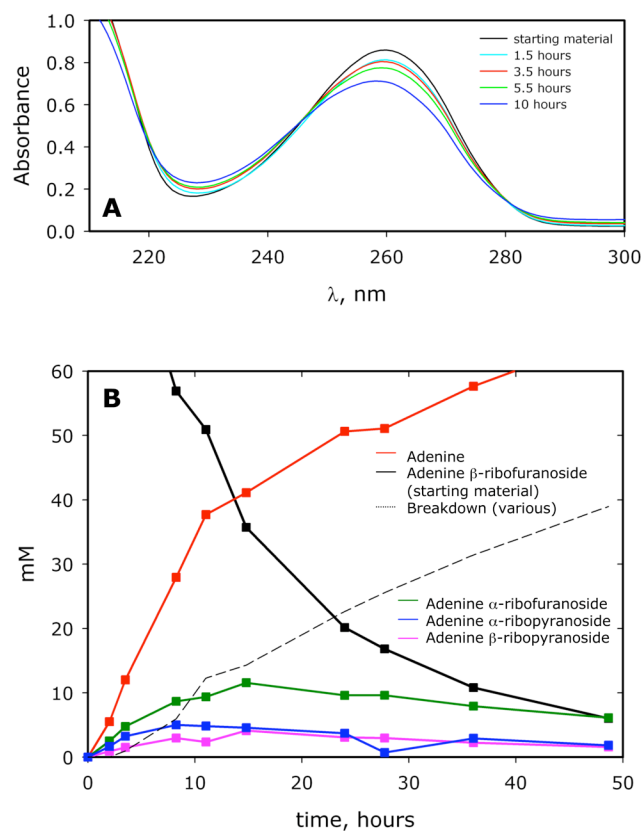


Figure 3. Time course for adenosine decomposition at 150 °C and pH 7.0. (A) Adenine ($\lambda_{\text{max}} = 261$) and adenosine ($\lambda_{\text{max}} = 260$) monitored with UV spectroscopy. The UV spectra have isosbestic points at 220, 245, and 280 nm. (B) The relative concentrations of adenine β -ribofuranoside (starting material, black), adenine (red), adenine α -ribofuranoside (green), adenine α -ribofuranoside (blue), adenine β -ribofuranoside (pink), and assorted breakdown products (dashed line).

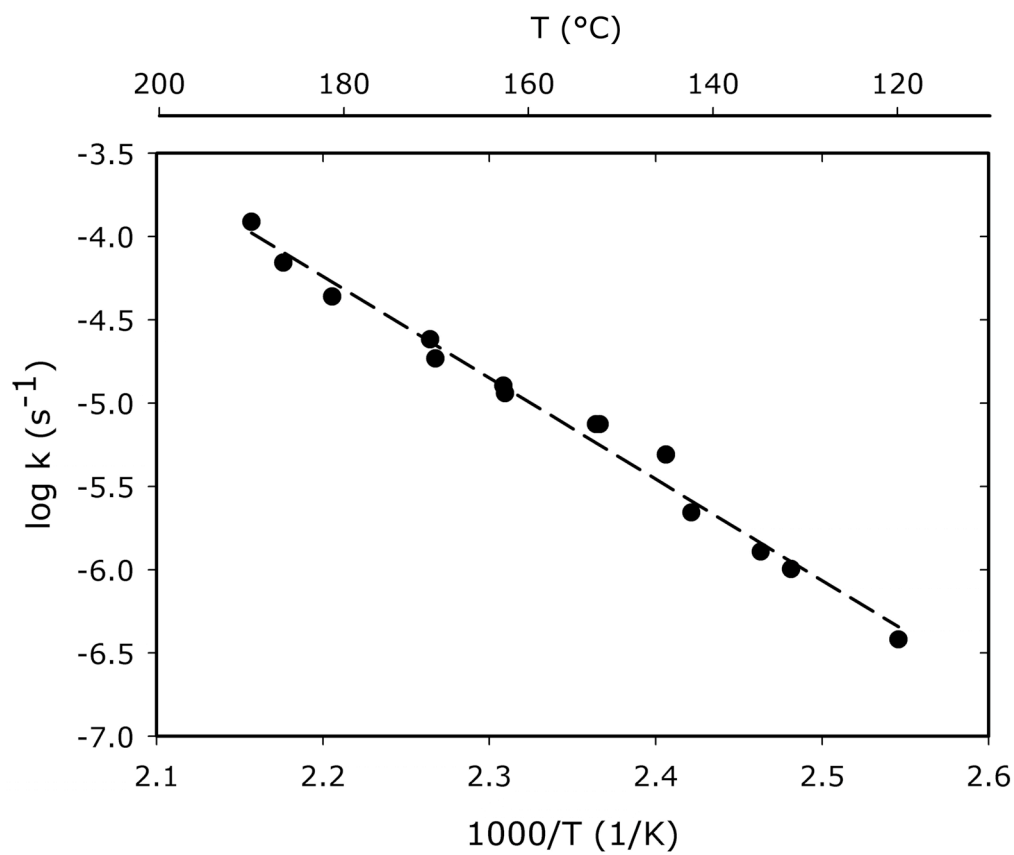
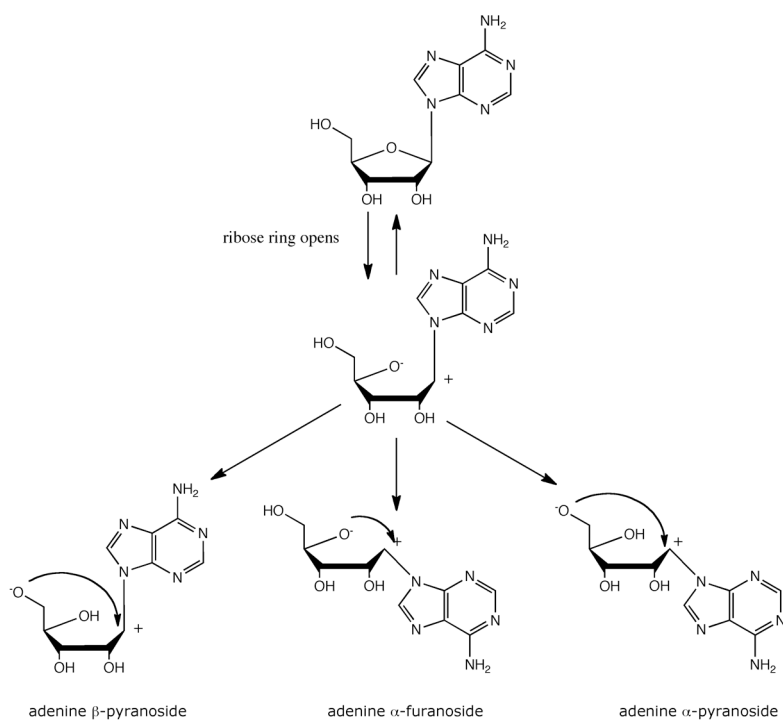


Figure 4. Arrhenius plot for cleavage of the adenosine glycosidic bond. Data were obtained between 110 and 190 ° C.

**Figure 5.**

A possible scheme for adenosine anomerization at pH 7. The ribose ring opens, forming a carbocation on C1'. In this intermediate structure, the adenine moiety, H1', and ribose are coplanar around C1', allowing isomerization to form α - and β -pyranosides or furanosides. This scheme is not intended to depict a mechanism or transition state structures; further kinetic analysis will be required to resolve those details.

Activation parameters and ^1H NMR chemical shifts for the formation of adenosine anomers α -ribofuranoside, β -ribofuranoside, and α -ribofuranoside.

Table 1

	^1H NMR			^{13}C NMR		activation parameters		
	H1'	H2	H8	C1'		ΔG^\ddagger	ΔH^\ddagger	TAS ‡
α -ribofuranoside ^a	6.34 d	8.13 s	8.32 s	83.30		32.8 ± 0.4	23.9	-8.8
α -ribofuranoside	5.80 s	8.21 s	8.50 s	--		32.9 ± 0.2	25.6	-7.4
β -ribofuranoside ^b	5.68 d	8.12 s	8.23 s	79.05		31.9 ± 0.2	23.4	-8.6

^aNMR data consistent with chemical shifts reported in [22] and data obtained with an authentic sample.

^bNMR data consistent with chemical shifts (obtained in DMSO-d₆) reported in [15].

Table 2

Activation parameters and rate constants for adenosine glycosidic bond cleavage compared to the enzyme-catalyzed reaction.

	ΔG^\ddagger	ΔH^\ddagger	$T\Delta S^\ddagger$	$t_{1/2}$	k_{non}	k_{cat}	$k_{\text{cat}}/k_{\text{non}}$
adenosine	32.9 ± 0.3	28.0	-4.9	6000 yrs.	$3.7 (\pm 1.3) \times 10^{-12} \text{ s}^{-1}$	$18 \text{ s}^{-1} a$	4.9×10^{12}
2'-deoxy-adenosine [20]	30.9	27.1	-3.8	180 yrs.	$1.2 \times 10^{-10} \text{ s}^{-1}$	$0.2 \text{ s}^{-1} b$	$2.8 \times 10^8 c$

^a k_{cat} value for *Trypanosoma brucei* nucleoside ribohydrolase [6].

^b k_{cat} value for adenine mismatch specific glycosylase MutY from *E. coli* [23]. Data obtained at 37°C.

^c Rate enhancement calculated from rate constants at 37°C.